12

Modeling and Assessing of Omni-directional Robots with Three and Four Wheels

Hélder P. Oliveira, Armando J. Sousa, A. Paulo Moreira and Paulo J. Costa
Universidade do Porto, Faculdade de Engenharia
INESC-Porto – Instituto de Engenharia de Sistemas e Computadores do Porto
Portugal

1. Introduction

Robots with omni-directional locomotion are increasingly popular due to their enhanced mobility when compared with traditional robots. Their usage is more prominent in many robotic competitions where performance is critical, but can be applied in many others applications such as service robotics. Robots with omni-directional locomotion offer advantages in manoeuvrability and effectiveness. These features are gained at the expense of increased mechanical complexity and increased complexity in control. Traditional mechanical configuration for omni-directional robots are based on three and four wheels. With four motors and wheels, it is expected that the robot will have better effective floor traction (Oliveira et al., 2008), that is, less wheel slippage at the expense of more complex mechanics, more complex control and additional current consumption.
Common robotic applications require precise dynamical models in order to allow a precise locomotion in dynamical environments. Such models are also essential to study limitations of mechanical configurations and to allow future improvements of controllers and mechanical configurations.
The presented study is based on a single prototype that can have both configurations, that is, the same mechanical platform can be used with three wheels and then it can be easily disassembled and reassembled with a four wheeled configuration. A mathematical model for the motion of the robot was found using various inertial and friction parameters. The motion analysis includes both kinematical and dynamical analysis.

1.1 Context

Robots with omni-directional locomotion are holonomic and they are interesting because they allow greater manoeuvrability and efficiency at the expense of some extra complexity. One of the most frequent solutions is to use some kind of variation of the Mecanum wheels proposed by (Diegel et al., 2002) and (Salih et al., 2006).
Omni-directional wheel design is quite delicate and different wheels exhibit very different performances. Wheel construction is often application specific and the presented work uses the wheels shown in Fig. 1. These wheels are built in-house for several demanding applications. The prototype used in the experiments uses four wheels of this kind to achieve

omni-directional locomotion. A robot with four wheels is expected to have more traction than its three wheeled counterpart. In both configurations the motor plus wheel assemblies are identical to the photograph seen in Fig. 2.

Fig. 1. 5DPO omni-directional wheel

Fig. 2. Motor and wheel

A robot with three or more motorized wheels of this kind can have almost independent tangential, normal and angular velocities (holonomic property). Dynamical models for this kind of robots are not very common due to the difficulty in modeling the several internal frictions inside the wheels, making the model somewhat specific to the type of wheel being used (Oliveira et al., 2008) and (Williams et al., 2002).
Frequent mechanical configurations for omni-directional robots are based on three and four wheels. Three wheeled systems are mechanically simpler but robots with four wheels have more acceleration with the same kind of motors. Four wheeled robots are expected to have better effective floor traction, that is, less wheel slippage - assuming that all wheels are pressed against the floor equally. Of course four wheeled robots also have a higher cost in equipment, increased energy consumption and may require some kind of suspension to distribute forces equally among the wheels.

(a) Three wheeled configuration

(b) Four wheeled configuration

Fig. 3. Configurations for the prototype

In order to study and compare the models of the three and four wheeled robots, a single prototype was built that can have both configurations, that is, the same mechanical platform

can be used with three wheels and then it can be disassembled and reassembled with a four wheel configuration, see Fig. 3.
Data from experimental runs is taken from overhead camera, see Fig. 4. The setup is taken from the heritage of the system described in (Costa et al., 2000) that currently features 25 frames/second, one centimeter accuracy in position (XX and YY axis) and about three degrees of accuracy in the heading of the robot.

Fig. 4. Image from overhead camera

In order to increase the performance of robots, there were some efforts on the studying their dynamical models (Campion et al., 1996), (Conceicao et al., 2006), (Khosla, 1989), (Tahmasebi et al., 2005), (Williams et al., 2002) and kinematic models (Campion et al., 1996), (Leow et al. 2002), (Loh et al. 2003), (Muir & Neuman, 1987), (Xu et al., 2005). Models are based on linear and non linear dynamical systems and the estimation of parameters has been the subject of continuing research (Conceicao et al., 2006), (Oliveira et al., 2008) and (Olsen and Petersen, 2001). Once the dynamical model is found, its parameters have to be estimated. The most common method for identification of robot parameters are based on the Least Squares Method and Instrumental Variables (Astrom & Wittenmark, 1984). However, the systems are naturally non-linear (Julier & Uhlmann, 1997), the estimation of parameters is more complex and the existing methods (Ghahramani & Roweis, 1999), (Gordon et al., 1993), (Tahmasebi et al., 2005) have to be adapted to the model's structure and noise.

2. Mechanical Configurations

Fig. 5 and Fig. 6 present the configuration of the three and four wheeled robots respectively, as well as all axis and relevant forces and velocities of the robotic system. The three wheeled system features wheels separated by 120º degrees, and the four wheeled by 90º degrees.

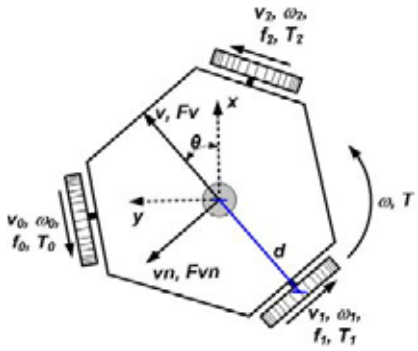

Fig. 5. Three wheeled robot

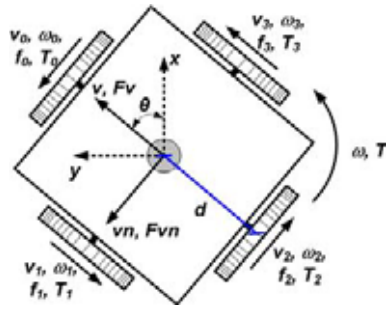

Fig. 6. Four wheeled robot

Fig. 5 and Fig. 6 show the notation used through-out this paper, detailed as follows:

- x, y, θ - Robot's position (x,y) and θ angle to the defined front of robot;
- d [m] - Distance between wheels and center robot;
- v_0, v_1, v_2, v_3 [m/s] - Wheels linear velocity;
- ω_0, ω_1, ω_2, ω_3 [rad/s] - Wheels angular velocity;
- f_0, f_1, f_2, f_3 [N] - Wheels traction force;
- T_0, T_1, T_2, T_3 [Nm] - Wheels traction torque;
- v, vn [m/s] - Robot linear velocity;
- ω [rad/s] - Robot angular velocity;
- F_v, F_{vn} [N] - Robot traction force along v and vn;
- T [Nm] - Robot torque (respects to ω).

The reader should be aware that in omni-directional robotics, the front of the robot is arbitrarily defined according to the intuitive notion of the robot mechanics. Of course, the v direction follows the front of the robot and the vn direction is orthogonal.

3. Motion Analysis and Model Determination

3.1 Kinematic model

In order to find motion models for a surface vehicle, the pose of the vehicle must be identified as (x, y, θ) and associated velocities are $v_x(t)=\frac{dx(t)}{dt}$, $v_y(t)=\frac{dy(t)}{dt}$, $\omega(t)=\frac{d\theta(t)}{dt}$.

The following text uses the notation presented in Fig. 5 and Fig. 6, where the defined "front" also defines the v direction and its orthogonal vn direction.

Equation (1) allows the transformation from linear velocities v_x and v_y on the static (world) axis to linear velocities v and vn on the robot's axis.

$$\begin{bmatrix} v(t) \\ vn(t) \\ \omega(t) \end{bmatrix} = \begin{bmatrix} \cos(\theta(t)) & \sin(\theta(t)) & 0 \\ -\sin(\theta(t)) & \cos(\theta(t)) & 0 \\ 0 & 0 & 1 \end{bmatrix} \cdot \begin{bmatrix} v_x(t) \\ v_y(t) \\ \omega(t) \end{bmatrix} \tag{1}$$

3.1.1 Three Wheeled Robot

Wheel velocities v_0, v_1 and v_2 are related with robot's velocities v, vn and ω as described by equation (2).

$$\begin{bmatrix} v_0(t) \\ v_1(t) \\ v_2(t) \end{bmatrix} = \begin{bmatrix} -\sin(\pi/3) & \cos(\pi/3) & d \\ 0 & -1 & d \\ \sin(\pi/3) & \cos(\pi/3) & d \end{bmatrix} \cdot \begin{bmatrix} v(t) \\ vn(t) \\ \omega(t) \end{bmatrix} \tag{2}$$

Applying the inverse kinematics is possible to obtain the equations that determine the robot velocities related with the wheels velocities. Solving in order of v, vn and ω, the following can be found:

$$v(t) = \left(\frac{\sqrt{3}}{3}\right) \cdot (v_2(t) - v_0(t)) \tag{3}$$

$$vn(t) = \left(\frac{1}{3}\right) \cdot (v_2(t) + v_0(t)) - \left(\frac{2}{3}\right) \cdot v_1(t) \tag{4}$$

$$\omega(t) = \left(\frac{1}{3 \cdot d}\right) \cdot (v_0(t) + v_1(t) + v_2(t)) \tag{5}$$

3.1.2 Four Wheeled Robot

The relationship between the wheels velocities v_0, v_1, v_2 and v_3, with the robot velocities v, vn and ω is described by equation (6).

$$\begin{bmatrix} v_0(t) \\ v_1(t) \\ v_2(t) \\ v_3(t) \end{bmatrix} = \begin{bmatrix} 0 & 1 & d \\ -1 & 0 & d \\ 0 & -1 & d \\ 1 & 0 & d \end{bmatrix} \cdot \begin{bmatrix} v(t) \\ vn(t) \\ \omega(t) \end{bmatrix} \tag{6}$$

It is possible to obtain the equations that determine the robot velocities related with wheels velocity but the matrix associated with equation (6) is not square. This is because the system is redundant. It can be found that:

$$v(t) = \left(\frac{1}{2}\right) \cdot (v_3(t) - v_1(t)) \tag{7}$$

$$vn(t) = \left(\frac{1}{2}\right) \cdot (v_0(t) - v_2(t)) \tag{8}$$

$$\omega(t) = \left(\frac{1}{4 \cdot d}\right) \cdot (v_0(t) + v_1(t) + v_2(t) + v_3(t)) \tag{9}$$

3.2 Dynamic

The dynamical equations relative to the accelerations can be described in the following relations:

$$M \cdot \frac{dv(t)}{dt} = \sum F_v(t) - F_{Bv}(t) - F_{Cv}(t) \tag{10}$$

$$M \cdot \frac{dvn(t)}{dt} = \sum F_{vn}(t) - F_{Bvn}(t) - F_{Cvn}(t) \tag{11}$$

$$J \cdot \frac{d\omega(t)}{dt} = \sum T(t) - T_{B\omega}(t) - T_{C\omega}(t) \tag{12}$$

where the following parameters relate to the robot are:

- M [kg] - Mass;
- J [kgm^2] - Inertia moment;
- F_{Bv}, F_{Bvn} [N] - Viscous friction forces along v and vn;
- $T_{B\omega}$ [N m] - Viscous friction torque with respect to the robot's rotation axis;
- F_{Cv}, F_{Cvn} [N] - Coulomb frictions forces along v and vn;
- $T_{C\omega}$ [Nm] - Coulomb friction torque with respect to robot's rotation axis.

Viscous friction forces are proportional to robot's velocities, see Fig. 7, and such as:

$$F_{Bv}(t) = B_v \cdot v(t) \tag{13}$$

$$F_{Bvn}(t) = B_{vn} \cdot vn(t) \tag{14}$$

$$T_{B\omega}(t) = B_\omega \cdot \omega(t) \tag{15}$$

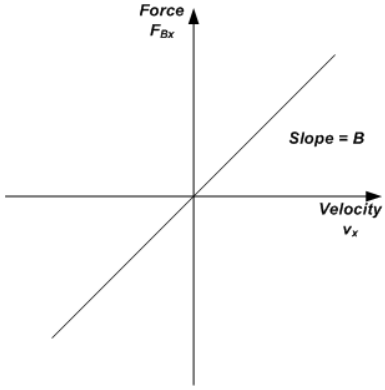

Fig. 7. Viscous friction

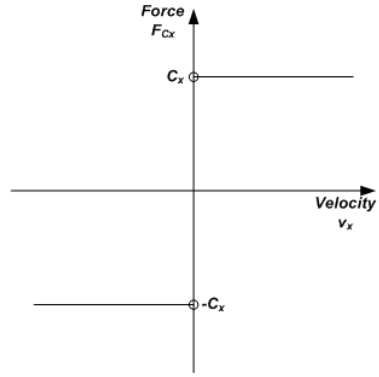

Fig. 8. Coulomb friction

where the following parameters relate to the robot as follows:

- B_v, B_{vn} [N/(m/s)] - Viscous friction coefficients for directions v and vn;
- B_ω [Nm/(rad/s)] - Viscous friction coefficient to ω.

The Coulomb friction forces are constant in amplitude, see Fig. 8.

$$F_{Cv}(t) = C_v \cdot sign(v(t)) \tag{16}$$

$$F_{Cvn}(t) = C_{vn} \cdot sign(vn(t)) \tag{17}$$

$$T_{C\omega}(t) = C_\omega \cdot sign(\omega(t)) \tag{18}$$

where the following parameters relate to the robot as follows:

- C_v, C_{vn} [N] - Coulomb friction coefficient for directions v e vn;
- C_ω [N m] - Coulomb friction coefficient for ω.

3.2.1 Three Wheeled Robot

The relationship between the traction forces and rotation torque of the robot with the traction forces on the wheels is described by the following equations:

$$\sum F_v(t) = (f_2(t) - f_0(t)) \cdot \sin\left(\frac{\pi}{3}\right) \tag{19}$$

$$\sum F_{vn}(t) = -f_1(t) + (f_2(t) + f_0(t)) \cdot \cos\left(\frac{\pi}{3}\right) \tag{20}$$

$$\sum T(t) = (f_0(t) + f_1(t) + f_2(t)) \cdot d \tag{21}$$

The traction force on each wheel is estimated by traction torque, which can be determined using the motor current, as described in the following equations:

$$f_j(t) = \frac{T_j(t)}{r} \tag{22}$$

$$T_j(t) = l \cdot K_t \cdot i_j(t) \tag{23}$$

where:

- l - Gearbox reduction;
- r [m] - Wheel radius;
- K_t [Nm/A] - Motor torque constant;
- i_j [A] - Motor current (j=motor number).

3.2.2 Four Wheeled Robot

$$\sum F_v(t) = f_3(t) - f_1(t) \tag{24}$$

$$\sum F_{vn}(t) = f_0(t) - f_2(t) \tag{25}$$

$$\sum T(t) = (f_0(t) + f_1(t) + f_2(t) + f_3(t)) \cdot d \tag{26}$$

As above, the traction force in each wheel is estimated using the wheels traction torque, which is determined by the motor current, using equations (22) and (23) where j=0,1,2,3.

3.3 Motor and Gearbox

The prototype uses brushless motors for the locomotion of the robot, photograph shown in Fig. 2. The used motors are from "Maxon Motor" (Maxon Motor, 2009), and the motor reference is "EC 45 flat 30 W". The main motor characteristics are: Nominal Power: 30W; Nominal Voltage: 12V; Nominal Current: 2.14A; Starting Current: 10A; Resistance phase to phase: 1.52 Ω; Terminal inductance phase to phase 0.56 mH; Torque constant 25.5 mNm/A; Speed constant 374 rpm/V; Mechanical time constant: 17.1 ms; Rotor inertia: 92.5 gcm^2 and a maximum efficiency of 77%.

The Gear-box Coupled to the motor is a "5:1 GS45", also from "Maxon Motor" (Maxon Motor, 2009), with a gear head of "Spur" type. The main characteristic are: Absolute Reduction: 51/10; Maximum mechanical efficiency of 90% and a mass inertia of 3.7 gcm^2.

This type of motors has been more common in the last years. The principal reason is the high performance when compared with others motors. These motors don't have mechanical switching, and this is the big difference to the common DC motors. The model for brushless motors is similar to the common DC motors, based on (Pillay & Krishnam, 1989).

$$u_j(t) = L \cdot \frac{di_j(t)}{dt} + R \cdot i_j(t) + K_v \cdot \omega_{mj}(t) \tag{27}$$

$$T_{mj}(t) = K_t \cdot i_j(t) \tag{28}$$

where:

- L [H] - Motor inductance;
- R [Ω] - Motor resistor;
- K_v [V/(rad/s)] - EMF motor constant;
- u_j [V] - Motor voltage (j=motor number);
- ω_{mj} [rad/s] - Motor angular velocity (j=motor number);
- T_{mj} [Nm] - Motor torque (j=motor number).

4. Parameter Estimation

The necessary variables to estimate the model parameters are motor current, robot position and velocity. Currents are measured by the drive electronics, position is measured by using external camera and velocities are estimated from positions.
The parameters that must be identified are the viscous friction coefficients (B_v, B_{vn}, B_ω), the Coulomb friction coefficients (C_v, C_{vn}, C_ω) and inertia moment J. The robot mass was measured, and it was 1.944 kg for the three wheeled robot and 2.340 kg for the four wheeled robot.

4.1 Experience 1 – Steady State Velocity

This method permits to identify the viscous friction coefficients B_ω and the Coulomb friction coefficients C_ω. The estimation of the coefficient according to velocity ω, was only implemented because inertia moment is unknown, and it is necessary to have an initial estimate of these coefficients. The experimental method relies on applying different voltages to the motors in order to move the robot according his rotation axis - the tests were made for positive velocities. Once reached the steady state, the robot's velocity ω and rotation torque T can be measured. The robot velocity is constant, so, the acceleration is null, and as such equation (12) can be re-written as follows:

$$\sum T(t) = B_\omega \cdot \omega(t) + C_\omega \tag{29}$$

This linear equation shows that it is possible to test different values of rotation velocities and rotation torques in multiple experiences and estimate the parameters.

4.2 Experience 2 – Null Traction Forces

This method allows for the estimation of the viscous friction coefficients (B_v, B_{vn}), the Coulomb friction coefficients (C_v, C_{vn}) and the inertia moment J. The experimental method

consists in measuring the robot acceleration and velocity when the traction forces were null. The motor connectors were disconnected and with a manual movement starting from a stable position, the robot was pushed through the directions v, vn and rotated according to his rotation axis. During the subsequent deceleration, velocity and acceleration were measured. Because the traction forces were null during the deceleration equations (10), (11) and (12) can be re-written as follows:

$$\frac{dv(t)}{dt} = -\frac{B_v}{M} \cdot v(t) - \frac{C_v}{M} \tag{30}$$

$$\frac{dvn(t)}{dt} = -\frac{B_{vn}}{M} \cdot vn(t) - \frac{C_{vn}}{M} \tag{31}$$

$$\frac{d\omega(t)}{dt} = -\frac{B_\omega}{J} \cdot v(t) - \frac{C_\omega}{J} \tag{32}$$

These equations are also a linear relation and estimation of all parameters is easier.
The inertia moment J is estimated using the values obtained in the previous section. To do this, equation (32) must be solved in order of J:

$$J = -\frac{\omega(t)}{d\omega(t)/dt} \cdot B_\omega - \frac{1}{d\omega(t)/dt} \cdot C_\omega \tag{33}$$

4.3 DC Motor Parameters

The previous electrical motor model (equation (27)) includes an electrical pole and a much slower, dominant mechanical pole - thus making inductance L value negligible. To determinate the relevant parameters K_v and R, a constant voltage is applied to the motor. Under steady state condition, the motor's current and the robot's angular velocity are measured. The tests are repeated several times for the same voltage, changing the operation point of the motor, by changing the friction on the motor axis.
In steady state, the inductance L disappears of the equation (27), being rewritten as follows:

$$u_j(t) = R \cdot i_j(t) + K_v \cdot \omega_{mj}(t) \tag{34}$$

As seen in equation (35), by dividing (34) by $i_j(t)$, a linear relation is obtained and thus estimation is possible.

$$\frac{u_j(t)}{i_j(t)} = R + K_v \cdot \frac{\omega_{mj}(t)}{i_j(t)} \tag{35}$$

5. Results

5.1 Robot Model

By combining previously mentioned equations, it is possible to show that model equations can be rearranged into a variation of the state space that can be described as:

$$\frac{dx(t)}{dt} = A \cdot x(t) + B \cdot u(t) + K \cdot sign(x) \tag{36}$$

$$x(t) = [v(t) \quad vn(t) \quad \omega(t)]^T \tag{37}$$

This formulation is interesting because it shows exactly which part of the system is non-linear.

5.1.1 Three Wheeled

Using equations on section 3.2, (19) to (23) and (34), the equations for the three wheeled robot model are:

$$A = diag(A_{11}, A_{22}, A_{33})$$

$$A_{11} = -\frac{3 \cdot K_t^2 \cdot l^2}{2 \cdot r^2 \cdot R \cdot M} - \frac{B_v}{M} \qquad A_{22} = -\frac{3 \cdot K_t^2 \cdot l^2}{2 \cdot r^2 \cdot R \cdot M} - \frac{B_{vn}}{M} \qquad A_{33} = -\frac{3 \cdot d^2 \cdot K_t^2 \cdot l^2}{r^2 \cdot R \cdot J} - \frac{B_\omega}{J} \tag{38}$$

$$B = \frac{l \cdot K_t}{r \cdot R} \begin{bmatrix} -\frac{\sqrt{3}}{2 \cdot M} & 0 & \frac{\sqrt{3}}{2 \cdot M} \\ \frac{1}{2 \cdot M} & \frac{1}{M} & \frac{1}{2 \cdot M} \\ \frac{d}{J} & \frac{d}{J} & \frac{d}{J} \end{bmatrix} \tag{39}$$

$$K = diag\left(-\frac{C_v}{M}, -\frac{C_{vn}}{M}, -\frac{C_\omega}{J}\right) \tag{40}$$

5.1.2 Four Wheeled

Using equations on section 3.2, (22) to (26) and (34), we get the following equations to the four wheeled robot model.

$$A = diag(A_{11}, A_{22}, A_{33})$$

$$A_{11} = -\frac{2 \cdot K_t^2 \cdot l^2}{r^2 \cdot R \cdot M} - \frac{B_v}{M} \qquad A_{22} = -\frac{2 \cdot K_t^2 \cdot l^2}{r^2 \cdot R \cdot M} - \frac{B_{vn}}{M} \qquad A_{33} = -\frac{4 \cdot d^2 \cdot K_t^2 \cdot l^2}{r^2 \cdot R \cdot J} - \frac{B_\omega}{J} \tag{41}$$

$$B = \frac{l \cdot K_t}{r \cdot R} \begin{bmatrix} 0 & -\frac{1}{M} & 0 & \frac{1}{M} \\ \frac{1}{M} & 0 & -\frac{1}{M} & 0 \\ \frac{d}{J} & \frac{d}{J} & \frac{d}{J} & \frac{d}{J} \end{bmatrix} \tag{42}$$

$$K = diag\left(-\frac{C_v}{M}, -\frac{C_{vn}}{M}, -\frac{C_\omega}{J}\right) \tag{43}$$

5.2 Experimental Data for Robot Model

5.2.1 Three Wheeled

Experience 1 was conducted using an input signal corresponding to a ramped up step, see Fig. 9. This way wheel sleeping was avoided, that is, wheel - traction problems don't exist.

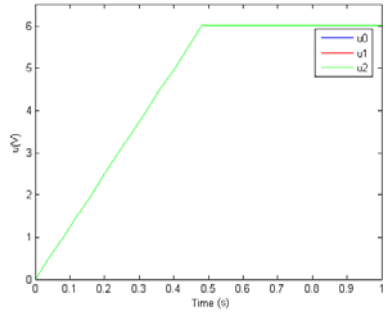

Fig. 9. Input voltage for the three wheeled robot

Table 1 and Fig. 10 shown the results for the three wheeled robot with experience 1.

u(V)	ω(rad/s)	T(Nm)
2	3.7062	0.1324
4	8.681	0.2319
6	13.4305	0.2789
8	18.3492	0.2972
10	21.8234	0.3662
12	26.2269	0.3971

Table 1. Experience 1 - Results for the three wheeled configuration

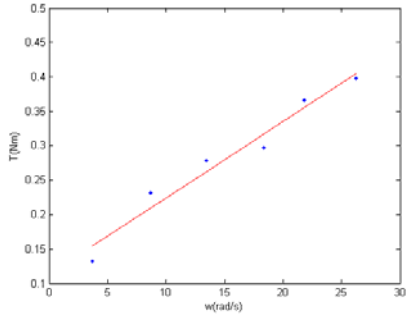

Fig. 10. Experience 1 - Results for the three wheeled configuration

The plots shown in Fig. 11 present the results obtained with experience 2.

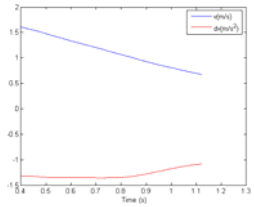
(a) Direction v

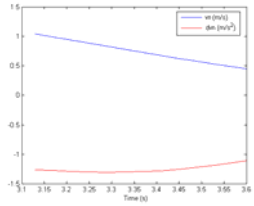
(b) Direction vn

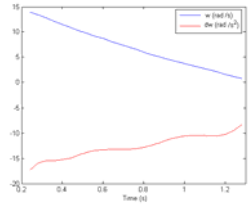
(c) Rotation axis

Fig. 11. Experience 2 – Velocity and acceleration for the three wheeled robot

5.2.2 Four Wheeled

Experience 1 was conducted using an input signal corresponding to a ramped up step, similar to the chart plotted in Fig. 9**.** This way wheel sleeping was avoided, that is, wheel - traction problems don't exist.

Table 2 and Fig. 12 show the results for the four wheeled robot with experience 1.

u(V)	ω(rad/s)	T(Nm)
2	3.7269	0.1491
4	8.7519	0.2645
6	13.519	0.3257
8	18.357	0.3352
10	22.4065	0.3966
12	27.1416	0.4513

Table 2. Experience 1 - Results for the four wheeled configuration

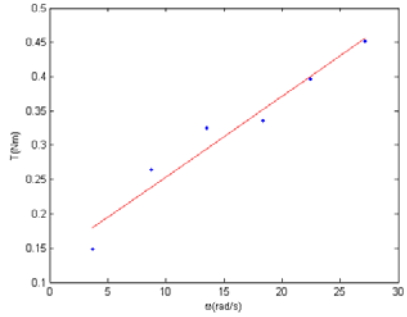

Fig. 12. Experience 1 - Results for the four wheeled configuration

The results obtained with experience 2 are shown in Fig. 13.

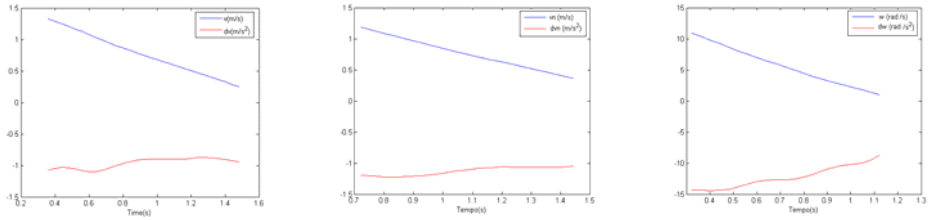

(a) Direction v (b) Direction vn (c) Rotation axis

Fig. 13. Experience 2 – Velocity and acceleration for the four wheeled configuration

5.2.3 Motor

The motor model was presented earlier in equation (34).

Experimental tests to the four motors were made to estimate the value of resistor R and the constant K_v. The numerical value of the torque constant K_t is identical to the EMF motor constant K_v.

Table 3 and Fig. 14 plots experimental runs regarding motor 0. Other motors follow similar behaviour.

u_0 (V)	i_0 (A)	ω_{m0} (rad/s)	ω_{m0}/i_0 ((rad/s)/A)	u_0/i_0 (Ω)
12	0.151	440.9	2910.1	79.2
12	0.831	345.7	415.7	14.4
12	0.425	402.1	945.0	28.2
12	0.456	397.0	870.3	26.3
12	0.715	360.5	503.6	16.7
12	0.641	371.5	579.6	18.7
12	1.164	301.0	258.4	10.3
12	0.272	423.7	1553.8	44.0
12	0.515	389.0	755.2	23.2
12	1.454	266.3	183.1	8.2

Table 3. Experimental tests with motor 0

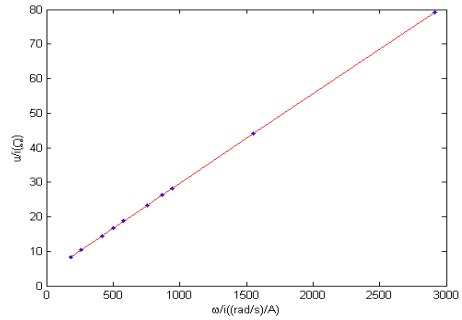

Fig. 14. Experimental tests for motor 0

5.3 Numerical Results

Table 4 presents the experimental results to the friction coefficients and inertial moment.

Parameters	3 wheels	4 wheels
J (kgm²)	0.015	0.016
B_v (N/(m/s))	0.503	0.477
B_{vn} (N/(m/s))	0.516	0.600
B_ω (Nm/(rad/s))	0.011	0.011
C_v (N)	1.906	1.873
C_{vn} (N)	2.042	2.219
C_ω (Nm)	0.113	0.135

Table 4. Friction coefficients and inertia moment

From the experimental runs from all 4 motors, the parameters found are K_v=0.0259 V/(rad/s) and R=3.7007 Ω.

To validate the model were made some experimental test on using a step voltage with a initial acceleration ramp, see Fig. 15.

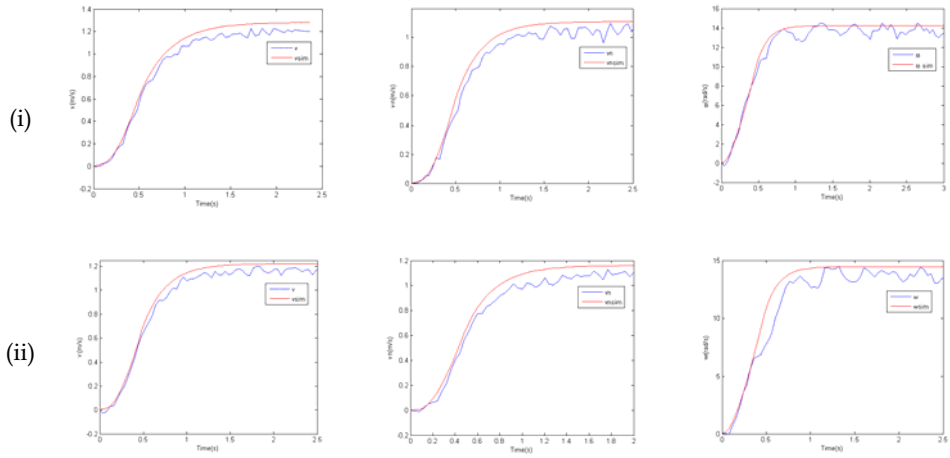

(a) Velocity along v (b) Velocity along vn (c) Angular velocity ω

Fig. 15. Experimental runs for initial model validation for the (i) three wheeled configuration and (ii) the four wheeled configuration

To evaluate the performance of the model, the real values of the velocities were compared to the estimated ones. The following numeric parameters are used to evaluate the adequacy of the model:

$$e_{\max} = \max\left|v(k) - v_{sim}(k)\right| \tag{44}$$

$$\overline{e} = \frac{1}{N} \cdot \sum_{i=1}^{N} e_i \tag{45}$$

$$\sigma = \sqrt{\frac{1}{N} \cdot \sum_{i=1}^{N} (e_i - \bar{e})^2} \tag{46}$$

where e_i represents the error in each instant.
The analysis of the errors of the experimental run shown in Fig. 15, in accordance to equations (44), (45) and (46) are analyzed later in Table 7.

5.4 Sensitivity Analysis

To understand which model parameters have more influence on the robot's dynamics, a comparison was made between the matrices of the models.
The model equation (36) is a sum of fractions. Analyzing the contribution of each parcel and of the variable portion within each fraction, a sensitivity analysis is performed, one estimated parameter at a time.

1. Matrix A, robot moving along v direction;
   - Three wheeled configuration:

$$\left(\frac{3 \cdot K_t^2 \cdot l^2}{2 \cdot r^2 \cdot R \cdot M}\right) = \frac{K_{a1}}{R} = 3.3110 \qquad \frac{B_v}{M} = K_{a2} \cdot B_v = 0.3245$$

   - Four wheeled configuration:

$$\left(\frac{2 \cdot K_t^2 \cdot l^2}{r^2 \cdot R \cdot M}\right) = \frac{K_{a1}}{R} = 3.6676 \qquad \frac{B_v}{M} = K_{a2} \cdot B_v = 0.2041$$

2. Matrix B and K, robot moving along v direction with constant voltage motor equal to 6V;
   - Three wheeled configuration:

$$\left(\frac{\sqrt{3} \cdot K_t \cdot l}{2 \cdot r \cdot R \cdot M}\right) \cdot 12 = \frac{K_b}{R} \cdot 12 = 5.7570 \qquad \frac{C_v}{M} = K_k \cdot C_v = 0.8728$$

   - Four wheeled configuration:

$$\left(\frac{K_t \cdot l}{r \cdot R \cdot M}\right) \cdot 12 = \frac{K_b}{R} \cdot 12 = 5.5227 \qquad \frac{C_v}{M} = K_k \cdot C_v = 0.7879$$

The same kind of analysis could be taken further by analyzing other velocities (vn and ω). Conclusions reaffirm that motor parameters have more influence in the dynamics than friction coefficients. This means that it is very important to have an accurate estimation of the motor parameters. Some additional experiences were designed to improve accuracy. The method used previously does not offer sufficient accuracy to the estimation of R. This parameter R is not a physical parameter and includes a portion of the non-linearity of the H bridge powering the circuit that, in turn, feeds 3 rapidly switching phases of the brushless motors used. In conclusion, additional accuracy in estimating R is needed.

5.5 Experience 3 – Parameter Estimation Improvement

The parameter improving experience was made using a step voltage with an initial acceleration ramp.

As seen in 5.1 the model was defined by the equation (36) and we can improve the quality of the estimation by using the Least Squares method (Gelb et al., 1974). The system model equation can be rewritten as:

$$y = \Theta_1 \cdot x_1 + \Theta_2 \cdot x_2 + \Theta_3 \cdot x_3 \tag{47}$$

where: x_1=x(t); x_2=u(t); x_3=1; y=dx(t)/dt.

The parameters Θ are estimated using:

$$\Theta = \left(x^T \cdot x\right)^{-1} \cdot x^T \cdot y \tag{48}$$

$$x = \left[x_1(1) \cdots x_1(n) \quad x_2(1) \cdots x_2(n) \quad x_3(1) \cdots x_3(n)\right]^T \tag{49}$$

Estimated parameters can be skewed and for this reason instrumental variables are used to minimize the error, with vector of states defined as:

$$z = \left[\bar{x}_1(1) \cdots \bar{x}_1(n) \quad x_2(1) \cdots x_2(n) \quad x_3(1) \cdots x_3(n)\right]^T \tag{50}$$

The parameters Θ are now calculated by:

$$\Theta = \left(z^T \cdot x\right)^{-1} \cdot z^T \cdot y \tag{51}$$

Three experiments were made for each configuration of three and four wheels, along v, vn and ω. For the v and vn experiments values C_v and C_{vn} are kept from previous analysis. For the ω experiment, the value of the R parameter used is the already improved version from previous v and vn experimental runs of the current section.

The numerical value of R for each motor was estimated for each motor and then averaged to find R=4.3111 Ω. The results are present on followings tables. Table 5 shows values estimated by the experiment mentioned in this section.

Parameters	3 wheels	4 wheels
J (kgm²)	0.0187	0.0288
B_v (N/(m/s))	0.5134	0.5181
B_{vn} (N/(m/s))	0.4571	0.7518
B_ω (Nm/(rad/s))	0.0150	0.0165
C_ω (Nm)	0.0812	0.1411

Table 5. Parameters estimated after experience 3

The final values for friction and inertial coefficients are averaged with results from all 3 experimental methods and the numerical values found are presented in Table 6.

Parameters	3 wheels	4 wheels
d (m)	0.089	
r (m)	0.0325	
l	5:1	
K_v (V/(rad/s))	0.0259	

R (Ω)	4.3111	
M (kg)	1.944	2.34
J (kgm²)	0.0169	0.0228
B_v (N/(m/s))	0.5082	0.4978
B_{vn} (N/(m/s))	0.4870	0.6763
B_ω (Nm/(rad/s))	0.0130	0.0141
C_v (N)	1.9068	1.8738
C_{vn} (N)	2.0423	2.2198
C_ω (Nm)	0.0971	0.1385

Table 6. Parameters of dynamical models

5.6 Model Validation Experiences

The models were validated with experimental tests on using a step voltage with an initial acceleration ramp. Fig. 16 show plots for the experimental runs.

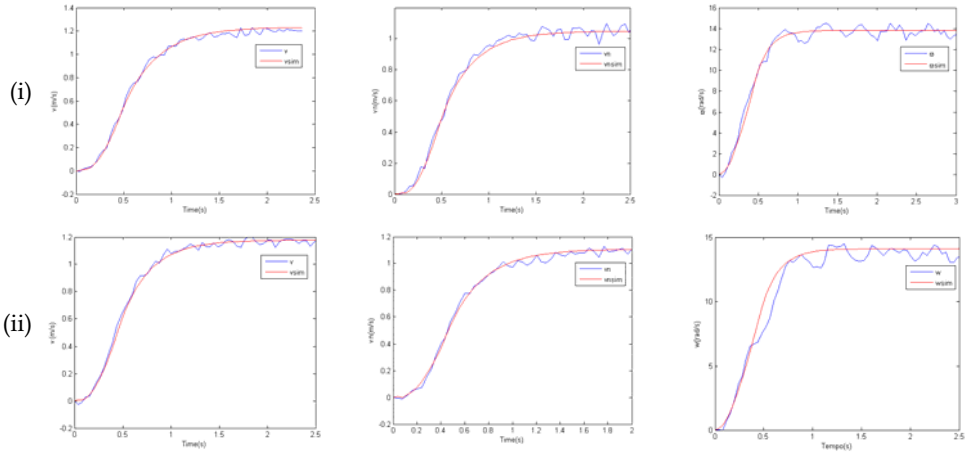

(a) Velocity along v (b) Velocity along vn (c) Angular velocity ω

Fig. 16. Experimental runs for final model validation for the (i) three wheeled configuration and (ii) four wheeled configuration

The analysis of the errors of the experimental runs shown in Fig. 16, in accordance to equations (44), (45) and (46) are presented in Table 7.

Confi-guration	Vels.	Initial			Final		
		e_{max}	$\bar{e}$	σ	e_{max}	$\bar{e}$	σ
Three wheeled	v	0.122	-0.059	0.034	0.067	-0.003	0.027
	vn	0.124	-0.055	0.032	0.051	0.016	0.023
	ω	1.699	-0.046	0.546	1.152	0.017	0.538
Four wheeled	v	0.096	-0.052	0.026	0.061	0.008	0.024
	vn	0.135	-0.070	0.034	0.068	-0.009	0.026
	ω	3.345	-0.919	0.852	2.504	-0.452	0.732

Table 7. Error analysis for initial and final estimated parameters (as shown I nFig. 15 and 16)

Fig. 17 shows the fit of the error of the initial experimental runs shown in Fig. 15 when compared to the fit of the errors for the final estimated parameters, as shown previously in Fig. 16. Clearly, the mean of the fits is closer to zero in the final parameters thus producing adequate model performance.

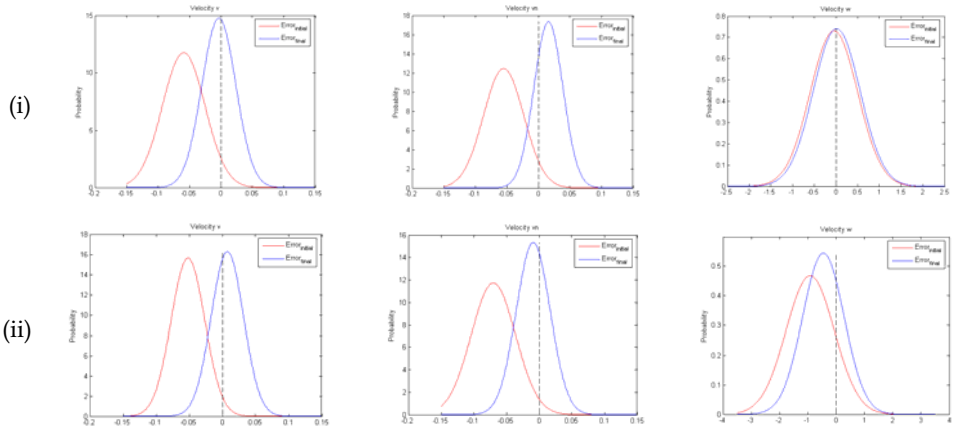

(a) Velocity along v (b) Velocity along vn (c) Angular velocity ω

Fig. 17. Comparison error fits for initial and final estimated parameters for the (i) three wheeled robot and the (ii) four wheeled

5.7 Assessment and Comparison of the Found Models

5.7.1 Preferential Directions

The models found, shown in section 5.1, prove that each mechanical configuration has different preferential direction at which the robot has maximum velocities, assuming ω=0. This fact can easily be ascertained by analysing the plots shown in Fig. 18 that occur periodically over π/3 for the three wheeled and periodically over π/2 for the four wheeled case.

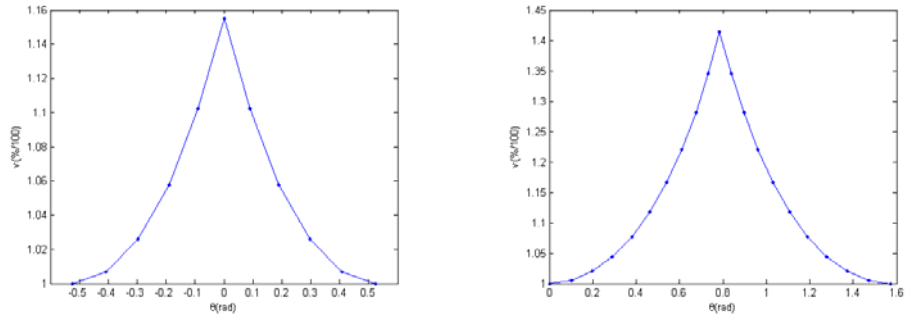

(a) Three wheeled configuration (b) Four wheeled configuration

Fig. 18. Normalized velocity variation over θ

The identified preferential directions are graphically identified in Fig. 19.

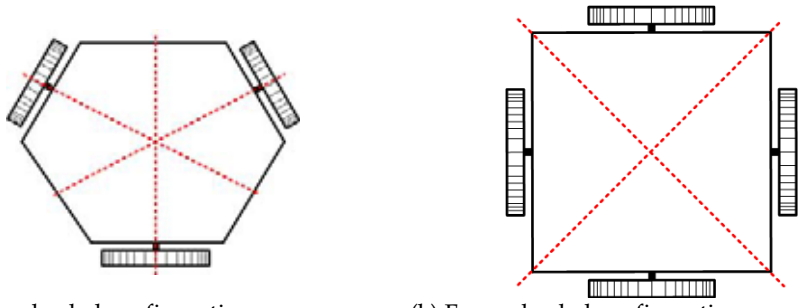

(a) Three wheeled configuration (b) Four wheeled configuration

Fig. 19. Preferential directions

5.7.2 Current Consumption

By observing Fig. 20 and Fig. 18, an interesting conclusion is revealed: on the three wheeled configuration the maximum velocity needs 8% less of the current than the current at the minimum velocity while the four wheeled configuration needs 90% more current when compared to the current needed for minimum velocity.

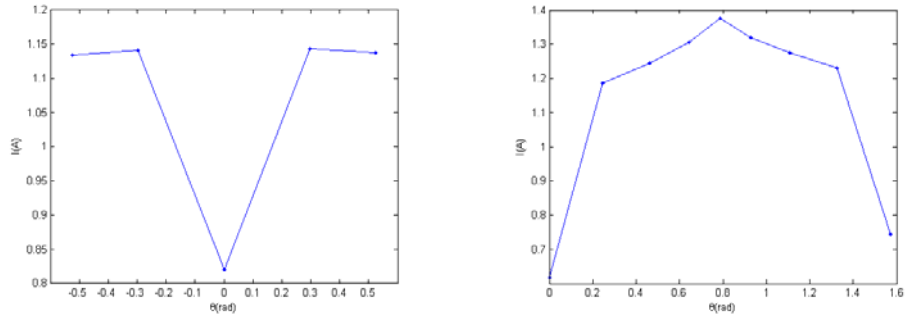

(a) Three wheeled configuration (b) Four wheeled configuration

Fig. 20. Current variation

5.7.3 Maximum Velocities

The plots shown in Fig. 21a) clearly show that the maximum velocity of the four wheeled configuration is larger than its three wheeled counterpart - the values are 3.58 m/s and 2.86 m/s respectively (at preferential directions). It thus seems natural that the accelerations shown in figure Fig. 21b) are also larger for the four wheeled configuration at the expense of a much larger current consumption, shown in Fig. 21c). This latest plots shows that roughly twice as much current is necessary to produce the previously mentioned 25% velocity increase. Fig. 21c) also shows that the sum of all the motor currents inside the robot with the four wheel configuration is about 11 A which is somewhat high and may be large enough to exceed the limits of the linearity of the system.

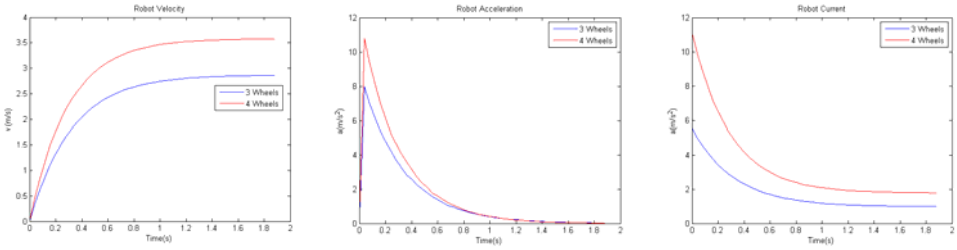

a) Velocities b) Accelerations c) Overall Currents

Fig. 21. Comparison of maximum velocities, associated accelerations and total currents

As explained earlier, the maximum speed varies with direction of the movement so it is interesting to observe the plot shown in Fig. 22 that comparatively predicts maximum speeds over the angle θ of the robot for both robotic configurations. It can be seen that the four wheeled configuration is frequently, but not always, faster than the three wheeled version. The three wheeled configuration has a smoother velocity profile whilst the four wheeled configuration has a large velocity gap in the preferential direction.

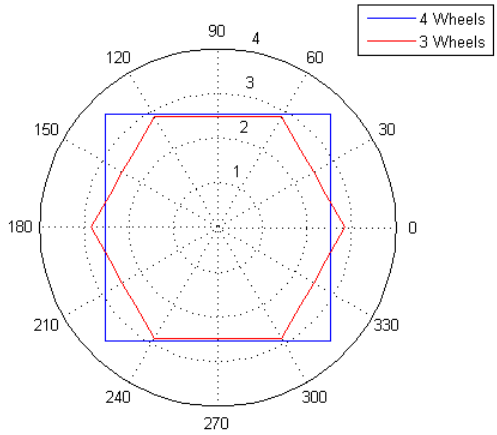

Fig. 22. Comparison of the velocity variation from the two platforms

6. Conclusions

This paper presents models for mobile omni-directional robots with three and four wheels. The derived model is non-linear but maintains some similarities with linear state space equations. Friction coefficients are most likely dependent on robot and wheels construction and also on the weight of the robot. The model is derived assuming no wheel slip as is interesting in most standard robotic applications.

A prototype that can have either three or 4 omni-directional wheels was used to validate the presented model. The test ground was smooth and carpeted. Experience data was gathered by overhead camera capable of determining position and orientation of the robot with good accuracy.

Experiences were made to estimate the parameters of the model for the prototypes. The accuracy of the presented model is discussed and the need for additional experiences is proved. The initial estimation method used two experiences to find all parameters but a third experience is needed to improve the accuracy of the most important model parameters. Sensitivity analysis shows that the most important model parameters concern motor constants.

Observing estimated model parameters, the four wheel robot has higher friction coefficients in the vn direction when compared to the v direction. This means of course higher maximum velocity for movement along v axis and higher power consumption for movements along the vn direction. This difference in performance points to the need of mechanical suspension to ensure even wheel pressure on the ground.

The found model was shown to be adequate for the prototypes in the several shown experimental runs.

From the derived models, some interesting conclusions were found. Firstly, it was proven that an omni-directional robot does not drive all directions with the same maximum velocity. As such, preferential directions for maximum velocities were found for each

configuration – these preferential directions are periodic and dependent on the wheel configuration. Another conclusion is that, as expected, the four wheeled configuration has a much, much larger current consumption when compared to the three wheeled version. It is interesting to note that the three wheeled configuration has smaller current consumption at its maximum velocity than that at its minimum velocity. Also interesting is the comparative plot of maximum velocities producible by the robot with each configuration for a given direction of movement. The three wheeled robot has small velocity gap at different directions of movement while important differences exist for the four wheeled version. It was also proven that, for a large portion of directions, the four wheeled version at maximum speed is faster, but not always! There is small portion of movement directions where the maximum velocity of the three wheeled configuration is superior to that of the four wheeled counterpart.

7. Future Work

The work presented is part of a larger study. Future work will include further tests with different prototypes including prototypes with suspension. The model can also be enlarged to include the limits for slippage and movement with controlled slip for the purpose of studying traction problems. Dynamical models estimated in this work can be used to study the limitations of the mechanical configuration and allow for future enhancements both at controller and mechanical configuration level. This study will enable effective full comparison of three and four wheeled systems.

8. References

Astrom, K. & Wittenmark, B. (1984), *Computer Controlled System – Theory and Design,* Prentice-Hall, Information and System Sciences Series, 1984.

Campion, G.; Bastin, G. & Dandrea-Novel, B. (1996), *Structural properties and classification of kinematic and dynamic models of wheeled mobile robots*, IEEE Transactions on Robotics and Automation, vol. 12(1), pp. 47-62, 1996.

Conceicao, A.; Moreira, A. & Costa, P. (2006), *Model Identification of a Four Wheeled Omni-Directional Mobile Robot*, Proceedings of the 7th Portuguese Conference on Automatic Control, Instituto Superior Tecnico, Lisboa, Portugal, 2006.

Costa, P.; Marques, P.; Moreira, A.; Sousa, A. & Costa, P. (2000), *Tracking and Identifying in Real Time the Robots of a F-180 Team*, in Manuela Veloso, Enrico Pagello and Hiroaki Kitano, editors. RoboCup-99: Robot Soccer World Cup III. Springer, LNAI, pp. 286-291, 2000.

Diegel, O.; Badve, A.; Bright, G.; Potgieter, J. & Tlale, S. (2002), *Improved Mecanum Wheel Design for Omni-directional Robots*, Proceedings of the Australasian Conference on Robotics and Automation, Auckland, 2002.

Gelb, A.; Kasper, J.; Nash, R.; Price, C. & Sutherland, A. (1974), *Applied Optimal Estimatio*n, MIT Press, 1974.

Ghaharamani, Z. & Roweis, S. (1999), *Learning Nonlinear Dynamical systems using an EM Algorithm*, In M. S. Kearns, S. A. Solla, D. A. Cohn, (eds) Advances in Neural Information Processing Systems, Cambridge, MA: MIT Press, vol. 11, 1999.

Gordon, N.; Salmond, D. & Smith, A. (1993), *Novel approach to nonlinear/non-Gaussian Bayesian state estimation*, IEE Proceedings-F on Radar and Signal Processing, vol. 140(2), pp. 107-113, 1993.

Julier, S. & Uhlmann, J. (1997), *A New Extension of the Kalman Filter to Nonlinear Systems*, Int. Symp. Aerospace/Defense Sensing, Simul. and Controls, Orlando, FL, 1997.

Khosla, P. (1989), *Categorization of parameters in the dynamic robot model*, IEEE Transactions on Robotics and Automation, vol. 5(3), pp. 261-268, 1989.

Leow, Y.; Low, K. & Loh, W. (2002), *Kinematic Modelling and Analysis of Mobile Robots with Omni-Directional Wheels*, Proceedings of the Seventh lnternational Conference on Control, Automation, Robotics And Vision, Singapore, 2002.

Loh, W.; Low, K. & Leow, Y. (2003), *Mechatronics design and kinematic modelling of a singularityless omni-directional wheeled mobile robot*, Proceedings of the IEEE International Conference on Robotics and Automation, vol. 3, pp. 3237-3242, 2003.

Maxon Motor (2009), *Maxon Motor Catalogue*, http://www.maxonmotor.com (visited April 2009)

Muir, P. & Neuman, C. (1987), *Kinematic modeling for feedback control of an omnidirectional wheeled mobile robot*, Proceedings of the IEEE International Conference on Robotics and Automation, vol. 4, pp. 1772-1778, 1987.

Oliveira, H.; Sousa, A.; Moreira, A. & Costa, P. (2008), *Dynamical models for omni-directional robots with 3 and 4 wheels*, Proceedings of the 5th International Conference on Informatics in Control, Automation and Robotics, pp. 189-196, 2008.

Olsen, M. & Petersen, H. (2001), *A new method for estimating parameters of a dynamic robot model*, IEEE Transactions on Robotics and Automation, vol. 17(1), pp. 95-100, 2001.

Pillay, P. & Krishnan, R. (1989), *Modeling, Simulation, and Analysis of Permanent-Magnet Motor Drives, Part 11: The Brushless DC Motor Drive*, IEEE transactions on Industry applications, vol. 25(2), pp. 274-279, 1989.

Salih, J.; Rizon, M.; Yaacob, S. ; Adom A.; & Mamat, M. (2006), *Designing Omni-Directional Mobile Robot with Mecanum Wheel*, American Journal of Applied Sciences, vol. 3(5), pp. 1831-1835, 2006.

Tahmasebi, A.; Taati, B.; Mobasser, F.; & Hashtrudi-Zaad, K. (2005), *Dynamic parameter identification and analysis of a PHANToM haptic device*, Proceedings of the IEEE Conference on Control Applications, pp. 1251-1256, 2005.

Williams, R.; Carter, B.; Gallina, P. & Rosati, G. (2002), *Dynamic model with slip for wheeled omnidirectional robots*, IEEE Transactions on Robotics and Automation, vol.18(3), pp. 285-293, 2002.

Xu, J.; Zhang, M. & Zhang, J. (2005), *Kinematic model identification of autonomous mobile robot using dynamical recurrent neural networks*, Proceedings of the IEEE International Conference Mechatronics and Automation, vol. 3, pp. 1447-1450, 2005.